Comparison of Thermal Imaging Systems Used in Thermography as a Non Destructive Testing Method for Composite Parts

Nathalie GERLACH, Haute Ecole Rennequin Sualem, Liège, Belgium

Abstract: Belgian Defense would like to use military thermal imagers to implement non destructive testing by thermography for airplanes and helicopters composite parts.
The choice of this camera is warranted by the analyse of parameters like NETD and MRTD and comparison with the same parameters for a popular civil camera.

1. Introduction

Belgian Defense has thermal imagers in great quantity (Sophie camera-Thalès). The use of these imagers to carry out non destructive testing by thermography would strongly reduce the cost of implementation of this technique within Defense. However, the choice of this material cannot be based only on economic criteria, it is also necessary that performances of the camera are at least equivalent to those of the civil cameras most usually used.
Thermal cameras can be classified according to their applications in two basic groups: monitoring cameras (imagers) and measurement cameras (radiometers). Monitoring cameras are mainly used in military applications to allow observation of battle field in darkness by creating a relative temperature distribution of the observed scene.
Measurement cameras are used for industrial applications for measurement without contact of temperature distribution at the surface of tested objects.
There are characteristics to describe camera performances. Subjective characteristics of image quality, noise and resolution are essential parameters of monitoring cameras while precision in absolute temperature is vital for measurement cameras.
Indeed, image subjective quality gives information on thermal camera capacity to detect, recognize and identify targets in various scenarios.
Noise characteristics provide information on camera response facing targets of variable size and temperature; noise limits camera sensitivity to detect targets of weak contrast.

2. MRTD

All measurement systems intended to test thermal cameras generate images of targets standards for the tested thermal camera. Thermal camera quality is given on the basis of targets standards image at the exit of the camera in the case of monitoring camera or of radiometric differences between real image and awaited image in case of measurement cameras .
Various types of targets are used according to characteristics of the camera to test. A target of

four bars is used for measurement of MRTD (minimum resolvable temperature difference). Slits are used for determination of resolution characteristics and crosses for geometrical characteristics.

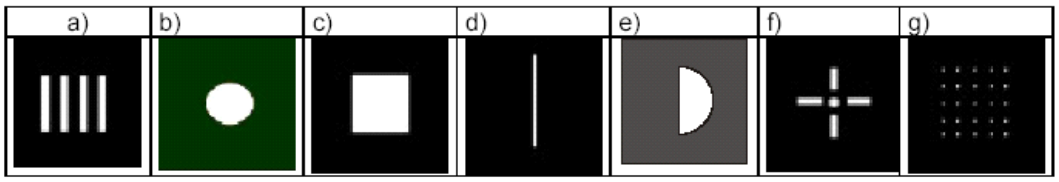

Figure 1: Different target types

MRTD is a subjective measurement of the infrared sensor sensitivity and its capacity to distinguish details. During this test, the difference in temperature between bars (a black body) and their combined (the target) increases until an observer can distinguish the four bars from the target. The critical difference in temperature is MRTD.

MRTD is regarded as the most important characteristic of monitoring cameras and makes it possible to compare a system with another (lower values of the MRTD indicate a better resolution).

2.1 Experimental device

We have two thermal cameras of which we wish to compare performances and more particularly MRTD.
The first one is a military monitoring camera Thalès using a FPA sensor (HgCdTe LWIR cooled by miniature Stirling cycle), the second one is a civil camera FLIR SC3000 (QWIP).

Figure 2: FLIR SC3000

Figure 3: Thalès Sophie camera

The rotary device consists of 12 targets with four bars of known space frequency placed opposite a black body.

Figure 4: rotating target

The space frequency is calculated by the formula:

$$F = \frac{10^{-3} D}{s}\left[\frac{cycle}{mrad}\right]$$

where F is space frequency
D is the distance between the target and the camera (m)
S is the distance centre to centre separating 2 bars in m (D>>>s).

Measurements are taken in a clean room controlled in temperature

2.3 Experimental results

MRTD Sophie Thales camera :

Target	Spatial frequency	MRTD+	MRTD-	meanMRTD
1	0,5	0,11	-0,07	0,092
2	0,98	0,2	-0,14	0,172
3	1,47	0,4	-0,33	0,366

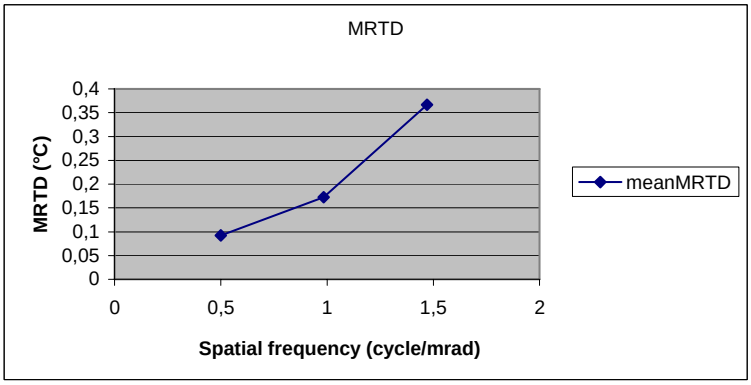

Figure 5 : MRTD vs spatial frequency

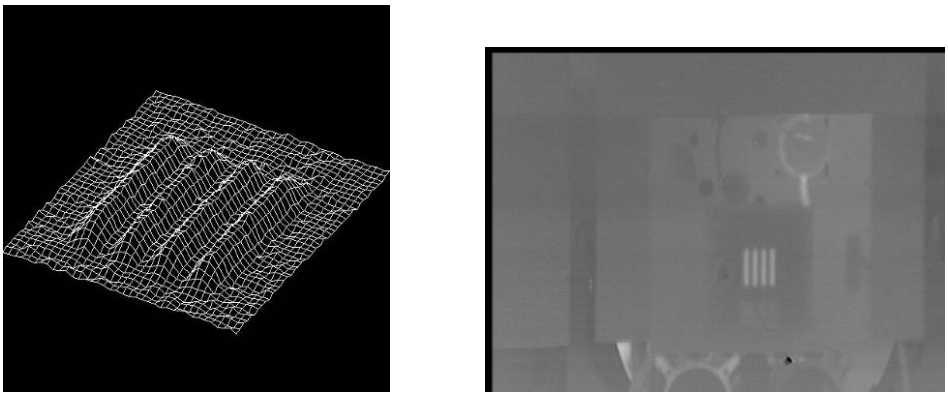

Figure 6 : limit differential temperature visualisation

MRTD FLIR SC3000 camera :

Cible	Spatial frequency	MRTD+	MRTD-	meanMRTD
1	0,25	0,07	-0,1	0,086
2	0,49	0,08	-0,5	0,357

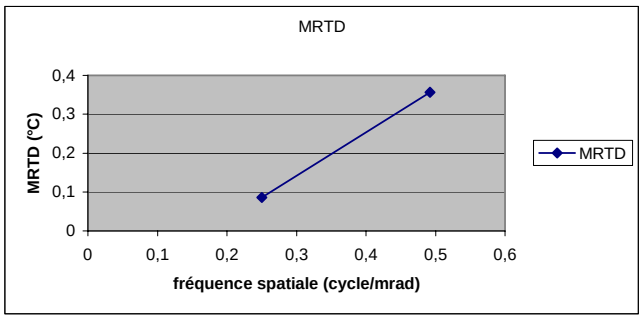

Figure 7 : MRTD versus spatial frequency

2.4 Conclusion

Sophie camera MRTD is significantly lower than that measured for civil camera FLIR. This observation was foreseeable since it is essential for a military camera to distinguish from the images of weak contrast whereas attention for a civil camera is mainly centered on reading precision.

3. Noise Equivalent Temperature Difference

Another important parameter which can be used to compare thermal cameras is NETD (noise equivalent temperature difference).
NETD provides an objective measurement of camera thermal sensitivity.
NETD is related to MRTD because an increase in NETD can mean loss of returned details of the image taken by the camera.
As NETD depends on the filmed object temperature, it is important to work in a clean room

controlled in temperature and to use black bodies of known temperature in order to compare various cameras.
We will use the black bodies provided with thermal Imager bench Thalès, these black bodies have a precision of 0,01°C.

NETD only is not sufficient to draw conclusions on the quality of sensors. It is also important to check if there is no variation of NETD according to the considered pixel.
If such a variation exists, we will check if this variation follows a Gaussian law around the mean value of the NETD of the whole image.
If the distribution moves away from a Gaussian distribution, the importance of observed dissymmetry also characterizes camera quality.

3.1 Determination of the intrinsic performances of a camera:

The thermal resolution of a camera is NETD, this parameter is the mean value of the deviation in time of the temperature of all pixels (window 100x100) deduced from the analysis of a thermal sequence of 40 images of a black body.

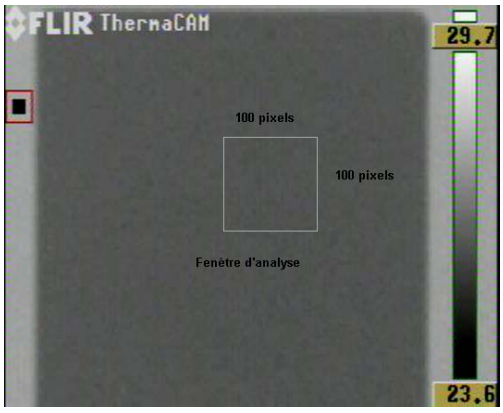

Figure 8 : Analyse window on black body

Figure 9 compares spatial distribution of standard temporal deviation of each pixel for FLIR SC3000 and the Thalès camera for a 25°C black body .
In this case, the analysis is carried out on a window of 100x100 pixels.
Under these conditions, the found mean NETD is closed to 30,6 mK for SC3000 and 78,92mK for Sophie .

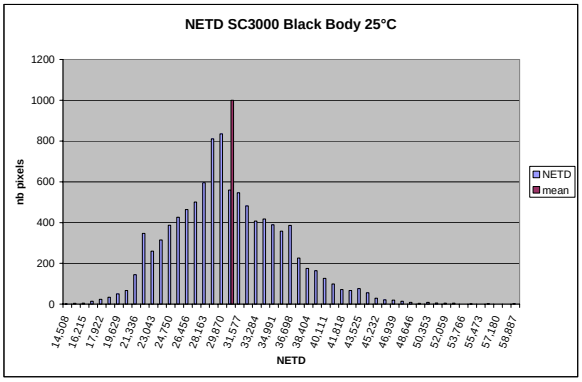

a. NETD SC3000 BB25

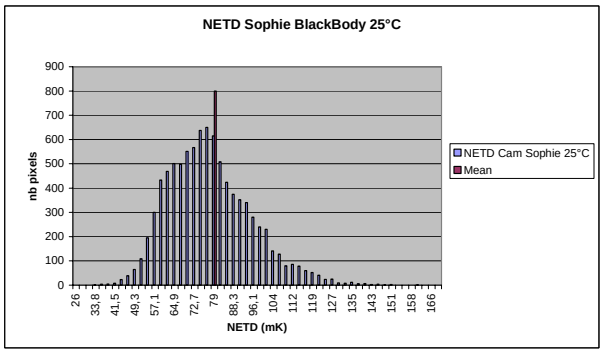

b. NETD Sophie BB25

Figure 9 : a. standard deviation 100x100 pixels- 25°C black body– SC3000 -Mean NETD is 30,6 mK.
b. standard deviation 100x100 pixels- 25°C blackbody – Sophie Mean NETD is 78,92 mK.

NETD distribution around the mean value is clearly dissymmetrical.

For SC3000, the NETD of each pixel varies from 14,5 mK to 58,88mK, 85% of the pixels posting a NETD lower than the central value of this interval (36,66mK).
For Sophie camera, the NETD of each pixel varies from 33,64 mK to 160,96 mK, 86% of the pixels have a NETD lower than the central value of this interval (97,3mK).

3.2 Influence of window size

Since there is a great variability in the values of NETD, it is interesting to check if this variability is associated with the pixel position in the image.
Calculation of mean NETD is carried out respectively on a centered window of 100x100 pixels then on windows accounting for 50% (70x70 pixels) then 25% (50x50 pixels) of this surface

Thales :

Fenêtre	Mean NETD (mK)
100x100	78,92
70x70	75,14
50x50	72,94

SC3000 :

Fenêtre	Mean NETD (mK)
100x100	30,62
70x70	30,47
50x50	30,41

The results show that the mean NETD is almost independent of the window used for FLIR SC3000 camera. For Sophie Thalès camera , the NETD varies slightly when the size of the window decreases, which tends to show that the sensor of this camera is more precise in the centre of the image than in periphery. If it were important to measure weak variations in temperature, it would be preferable, with this camera, to place observed object in the centre of the image.

For FLIR SC3000 camera, it appears that dissymmetry is not strongly influenced by the size of the selected window.

For all windows, there are as many pixels which have a NETD lower than the NETD corresponding to the maximum of distribution (29,87 mK) that pixels whose NETD is higher than the NETD of the maximum of distribution.

However, NETD lower than the NETD of the maximum of distribution vary from 14,5 mK to 29,87 mK (either a variability of 15,37 mK) whereas NETD higher than maximum vary from 29,87 mK to 54,62 mK (or a variability of 24,75 mK).

The same observation is valid for Sophie camera, there are as many pixels on both sides of the distribution maximum value (77,88 mK). Moreover, dissymmetry is still observable, NETD lower than the maximum of the distribution extend from 25,96 mK to 77,88 mK (either a variability of 51,96mK) while higher NETD extend from 77,88 mK to 160,98 mK (or 83,1mK).

Let us consider cumulative distribution of NETD for individual pixels (integral of distribution). y axis represents percentage of pixels whose NETD is lower or equal to NETD given by x axis.

For SC3000 camera , we notice that the percentage of pixels whose NETD is lower than the mean NETD is not significantly modified when the size of the window decreases.

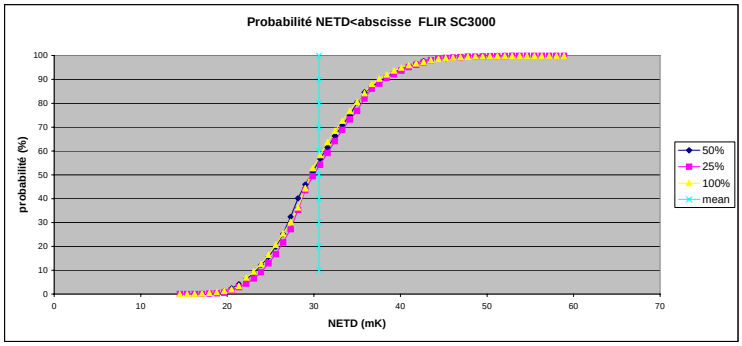

Figure 10 : NETD Cumulative probability for SC3000 camera

Let us call this PNEDTmean percentage. This parameter is the probability that a given pixel has a NETD≤meanNETD.

We can take this number like a characteristic of image quality. It is clear that image quality is not improved by window size reduction.

Same analysis on Sophie camera results is represented on the following figure:

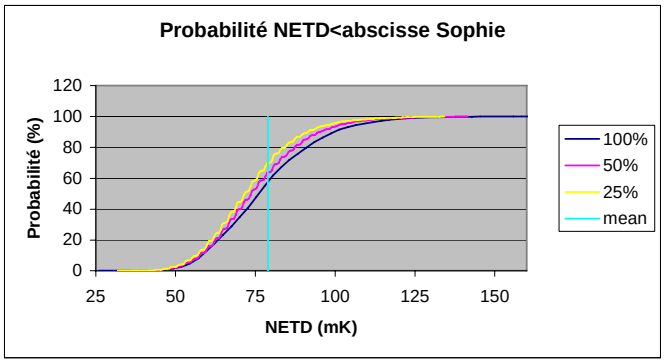

Figure 11: NETD cumulative probability for Sophie camera

It is observed, in accordance with the tendency already observed for mean NETD, that there is a light difference between PNEDTmean percentage for various fenestrations. The window concentrated in sensor centre has a quality higher compared to broader fenestrations.

3.3 Conclusion

FLIR SC3000 sensor presents a mean NETD lower than the one of Sophie camera. This observation indicates that FLIR camera sensor is better to distinguish very weak thermal differences than Sophie camera.
However, the NETD mean values remain in the same order of magnitude.
Both sensors present a significant asymmetry. In both cases, sixty percents of pixels have a NETD lower than the mean NETD. As this probability can be regarded as a quality index of a sensor, that indicates that both sensors have, according to this criterion, an equivalent quality.
If SC3000 sensor quality is uniform, Thales camera quality is not identical in any point of the sensor. The centre of the sensor presents a NETD slightly lower than periphery and PNEDTmean increases when the window decreases.
Analysis of NETD thus states that SC3000 sensor has characteristics slightly better than that of Sophie camera (NETD mean value and uniformity on sensor).

4. Conclusions

MRTD and NETD analyses indicates than SC3000 camera sensor presents slightly better characteristics than Sophie camera sensor (NETD mean value and sensor uniformity).
But Sophie NETD remains lower than 80 mK. This camera is able to distinguish defects with thermal signature higher than this value. If heating is strong enough, deep defects (depth up to 3mm) are easily detected by military Sophie camera. A NETD higher than SC3000 NETD doesn't inhibit from using Sophie camera for non destructive testing.

References

[1] Garcia J., Hernandez N., Morales A., Servent R., Considerations of Thermographic Inspection Reliability of Aircraft Components, Proc. 8th ECNDT Barcelona, 2002

[2] Maldague X., Nondestructive testing handbook volume 3: Infrared and Thermal Testing, American Society for Nondestructive Testing, 2001.

[3] Maldague X., Theory and Practice of Infrared Technology for Non Destructive Testing, John-Wiley & Sons, 2001.

[4] Maldague X. And Vavilov V., Basics of Infrared Thermography, Quantitative Infrared Thermography QIRT'04..

[5] Zweschper Th., Dillenz A., Riegert G., Scherling D., Busse G., Lockin Thermography Methods For the NDT of CFRP Aircraft Components, Proc. 8th ECNDT Barcelona,2002.